

See discussions, stats, and author profiles for this publication at: <https://www.researchgate.net/publication/275220796>

Synthesis, Characterization, Crystal Structure and Antimicrobial Activity of Copper(II) Complexes with the Schiff Base Derived from 2-Hydroxy-4-Methoxybenzaldehyde

ARTICLE *in* MOLECULES · APRIL 2015

Impact Factor: 2.42 · DOI: 10.3390/molecules20045771

CITATIONS

2

READS

151

7 AUTHORS, INCLUDING:



Diana - Carolina Ilies

Carol Davila University of Medicine and Pha...

20 PUBLICATIONS 110 CITATIONS

SEE PROFILE



Sergiu Shova

Petru Poni Institute of Macromolecular Che...

214 PUBLICATIONS 1,758 CITATIONS

SEE PROFILE



Mihaela Badea

University of Bucharest

100 PUBLICATIONS 573 CITATIONS

SEE PROFILE



Gulea Aurelian

Moldova State University

74 PUBLICATIONS 594 CITATIONS

SEE PROFILE

Article

Synthesis, Characterization, Crystal Structure and Antimicrobial Activity of Copper(II) Complexes with the Schiff Base Derived from 2-Hydroxy-4-Methoxybenzaldehyde

Elena Pahonțu ¹, Diana-Carolina Ilieș ^{2,3,*}, Sergiu Shova ⁴, Codruța Paraschivescu ⁵, Mihaela Badea ², Aurelian Gulea ⁶ and Tudor Roșu ²

¹ Inorganic Chemistry Department, Faculty of Pharmacy, University of Medicine and Pharmacy “Carol Davila”, 6 Traian Vuia Street, 020956 Bucharest, Romania;

E-Mail: elenaandmihaela@yahoo.com

² Inorganic Chemistry Department, Faculty of Chemistry, University of Bucharest,

23 Dumbrova Rosie Street, 020462 Bucharest, Romania; E-Mails: e_m_badea@yahoo.com (M.B.); t_rosu0101@yahoo.com (T.R.)

³ Organic Chemistry Department, Faculty of Pharmacy, University of Medicine and Pharmacy “Carol Davila”, 6 Traian Vuia Street, 020956 Bucharest, Romania

⁴ Institute of Macromolecular Chemistry “Petru Poni”, 41A Grigore Ghica Voda Alley, 700487 Iasi, Romania; E-Mail: shova@icmpp.ro

⁵ Organic Chemistry Department, Faculty of Chemistry, University of Bucharest, 90-92 Panduri Street, 050663 Bucharest, Romania; E-Mail: c.paraschivescu@gmail.com

⁶ Coordination Chemistry Department, Moldova State University, 60 Mateevici Street, 2009 Chisinau, Moldova; E-Mail: dociu1946@yahoo.com

* Author to whom correspondence should be addressed; E-Mail: ilies_diana@hotmail.com; Tel.: +40-075-402-5528; Fax: +40-021-318-0750.

Academic Editor: Derek J. McPhee

Received: 2 February 2015 / Accepted: 24 March 2015 / Published: 2 April 2015

Abstract: A novel Schiff base, ethyl 4-[(E)-(2-hydroxy-4-methoxyphenyl)methylene-amino]benzoate (**HL**), was prepared and structurally characterized on the basis of elemental analyses, ¹H NMR, ¹³C NMR, UV-Vis and IR spectral data. Six new copper(II) complexes, [Cu(L)(NO₃)(H₂O)₂] (**1**), [Cu(L)₂] (**2**), [Cu(L)(OAc)] (**3**), [Cu₂(L)₂Cl₂(H₂O)₄] (**4**), [Cu(L)(ClO₄)(H₂O)] (**5**) and [Cu₂(L₂S)(ClO₄)(H₂O)]ClO₄·H₂O (**6**) have been synthesized. The characterization of the newly formed compounds was done by IR, UV-Vis, EPR, FAB mass spectroscopy, elemental and thermal analysis, magnetic

susceptibility measurements and molar electric conductivity. The crystal structures of Schiff base and the complex $[\text{Cu}_2(\text{L}_2\text{S})(\text{ClO}_4)(\text{H}_2\text{O})]\text{ClO}_4 \cdot \text{H}_2\text{O}$ (**6**) have been determined by single crystal X-ray diffraction studies. Both copper atoms display a distorted octahedral coordination type $[\text{O}_4\text{NS}]$. This coordination is ensured by three phenol oxygen, two of which being related to the μ -oxo-bridge, the nitrogen atoms of the azomethine group and the sulfur atoms that come from the polydentate ligand. The *in vitro* antimicrobial activity against *Escherichia coli* ATCC 25922, *Salmonella enteritidis*, *Staphylococcus aureus* ATCC 25923, *Enterococcus* and *Candida albicans* strains was studied and compared with that of free ligand. The complexes **1**, **2**, **5** showed a better antimicrobial activity than the Schiff base against the tested microorganisms.

Keywords: Schiff bases; copper(II) complex; crystal structure; EPR spectra; antimicrobial activity

1. Introduction

The synthesis of new compounds that are used for the treatment of infections with less secondary effects is a biomedical problem [1,2]. Recently research has focused increasingly on the synthesis of transition metal complexes with Schiff-type ligands, due to the biological properties that they present. Many compounds derived from Schiff bases exhibit antibacterial, antifungal, antitumor and anti-HIV activities [3–14]. Schiff bases derived from salicylaldehyde represent an important class of ligands due to their ability to be used in various fields [15–19]. Having a high capacity chelating and redox potential the positive Cu^{2+} ion is biologically active, and participates in many processes in the body [20–22]. Copper complexes are also among the most potent antiviral, antitumor and anti-inflammatory agents [23]. In addition, it was found that most of benzocaine-containing compounds are biologically active. Recent research has demonstrated that, these derivatives exhibit antimicrobial activity against different species [24–26]. Based on these observations and considering research in this area in the present study, we report the synthesis, characterization, antimicrobial studies of some copper(II) complexes containing a Schiff base ligand derived from 2-hydroxy-4-methoxybenzaldehyde and ethyl-4-aminobenzoate, with a special impetus on ligand structural investigations. The crystal structures of ligand and complex **6** were studied by X-ray diffraction. The biological properties of these compounds was tested for their antibacterial and antifungal activities against *Escherichia coli* ATCC 25922, *Salmonella enteritidis*, *Staphylococcus aureus* ATCC 25923 and *Candida albicans* strains.

2. Results and Discussion

2.1. Chemistry

The Schiff base **HL** was prepared by refluxing in ethanol an equimolar mixture of 4-aminobenzoic acid ethyl ester with 2-hydroxy-4-methoxybenzaldehyde. The structure of the formed Schiff bases was established by IR, $^1\text{H-NMR}$ and $^{13}\text{C-NMR}$ spectroscopies and by X-ray crystallography. All compounds were synthesized by direct reaction between ligand and the corresponding metal salts,

while compound **6** was prepared by using a mixture of $\text{Cu}(\text{ClO}_4)_2 \cdot 6\text{H}_2\text{O}$ and **HL** with addition of NaSCN . All complexes are microcrystalline solids. Also, the melting point values are greater than 220°C . They are insoluble in organic solvents such as acetone and methanol, but soluble in DMF and DMSO. The molar conductivity values ($8\text{--}12 \text{ ohm}^{-1} \cdot \text{cm}^2 \cdot \text{mol}^{-1}$) of the complexes **1–5** in 10^{-3} M solution DMF show that they are non-electrolytes and **6** ($82 \text{ ohm}^{-1} \cdot \text{cm}^2 \cdot \text{mol}^{-1}$) is an electrolyte [27].

The thermal decompositions of the complexes **1–4** were studied by thermogravimetry (TG). The TG and TGD curves have three or four stages of mass loss. The first weight loss step correspond of two and four water molecules respectively, per one molecule of complex (7.26% for complex **1**, 8.63% for complex **4**). Thermal analyses data reveal that compounds **2** and **3** not are hydrated. The final residue was analyzed by IR spectroscopy, which confirms the formation of CuO (Figure S1).

The elemental analyses data of the Schiff base and complexes (reported in Section 3) are in agreement with structure of the ligand (Figure 1) and with structures of the complexes (Figure 2).

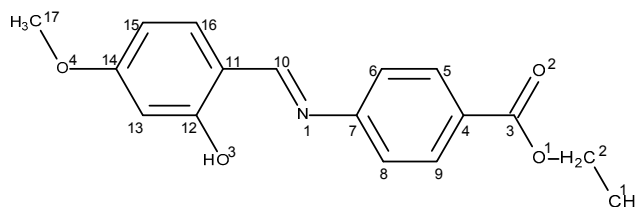


Figure 1. Schiff base ligand (**HL**).

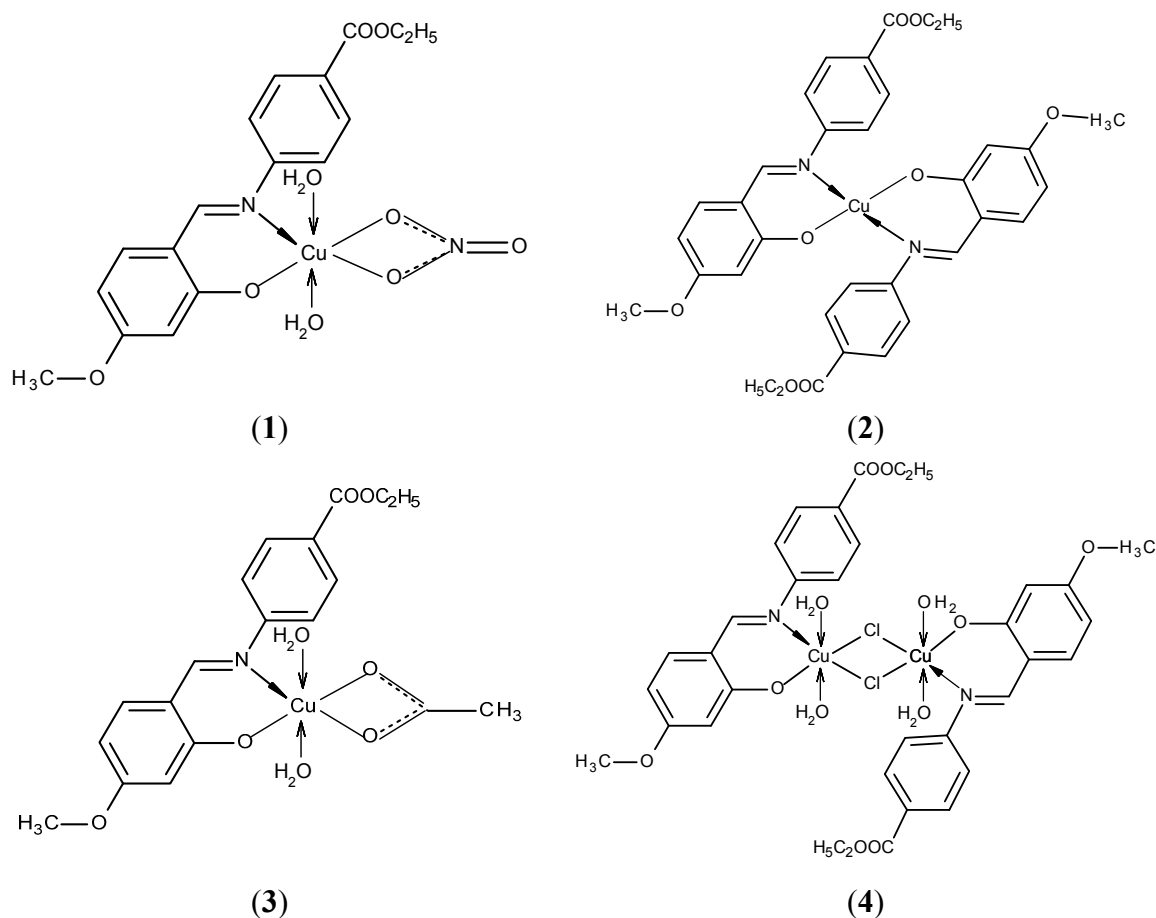
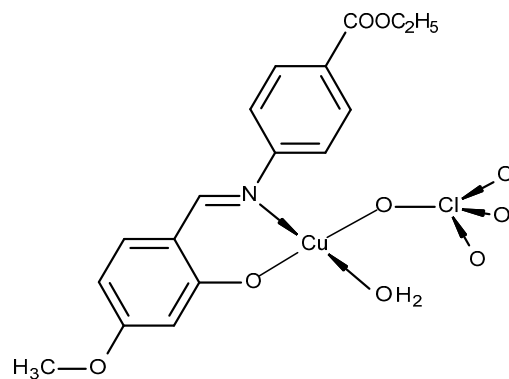


Figure 2. Cont.

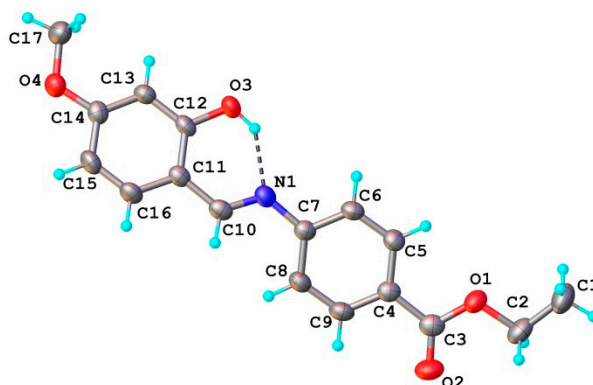


(5)

Figure 2. Proposed structures for the copper(II) complexes 1–5.

2.1.1. Structural characterization of (HL)

The ligand **HL** structure is shown in Figure 3. The planar configuration of **HL** molecule is stabilized by an intra-molecular O-H \cdots N hydrogen bond which is observed in the majority of Schiff base ligands obtained from 2-hydroxybenzaldehyde [28].

**Figure 3.** X-ray molecular structure of (**HL**). Thermal ellipsoids are drawn at 50% probability level. H-bond parameters: O3–H \cdots N1 [O3–H 0.86 Å, H \cdots N1 1.87 Å, O3 \cdots N1 2.602(2) Å, O3–H \cdots N1 140.7°].

The crystal packing of **HL** is stabilized by π - π stacking and C-H \cdots O cooperative interactions. *Cg*1 (the centroid of the C-C9 ring) exhibits a stacking interaction with *Cg*2 (the centroid of the C11-C16 ring) of the adjacent molecule, related by two-fold axis, with a centroid-to-centroid distance of 3.851(4) Å. The formed dimeric units (Figure 4) are further associated due to the presence of weak C-H \cdots O intermolecular interactions resulting into the formation of two-dimensional supramolecular ribbons, as the main crystal structure packing motif, depicted in Figure 5.

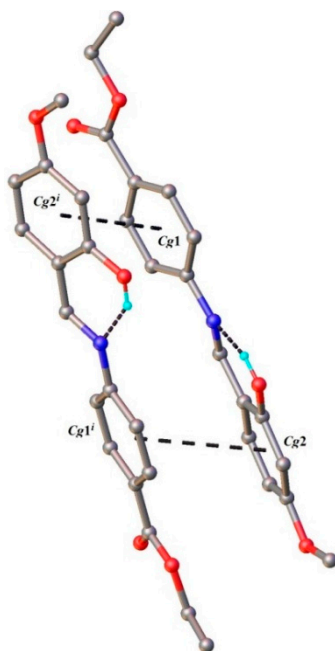


Figure 4. π - π staking interactions in the crystal structure (**HL**).

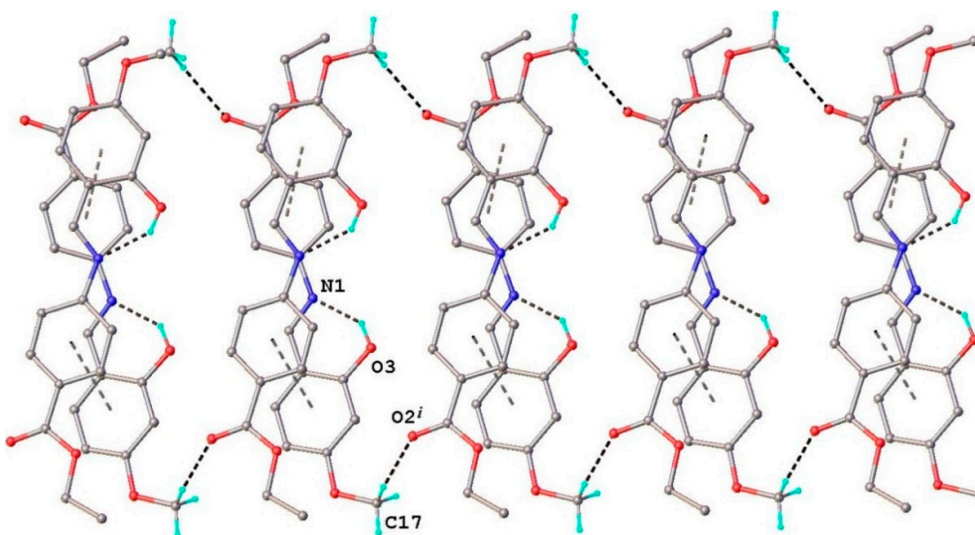


Figure 5. View of the supramolecular ribbon in the crystal structure (**HL**). C17–H \cdots O2 [C17–H 0.96 Å, H \cdots O2 2.44 Å, C17 \cdots O2($-x$, $-1 + y$, $1.5 - z$) 3.378(4) Å, C17–H \cdots O2 164.4°].

2.1.2. Structural Characterization of $[\text{Cu}_2(\text{L}_2\text{S})_2(\text{ClO}_4)(\text{H}_2\text{O})]\text{ClO}_4 \cdot \text{H}_2\text{O}$ (**6**)

Selected bond lengths and angles for **HL** are presented in Tables 1 and 2.

Complex **6** has a crystal structure formed from the complex binuclear cations $[\text{Cu}_2(\text{L}_2\text{S})_2(\text{ClO}_4)(\text{H}_2\text{O})]^+$, ClO_4^- anions and H_2O as solvate molecules 1:1:1 molar ratio. The structure of the complex cation is presented in Figure 6.

Table 1. Selected bond lengths (Å) and bond angles (°) for HL.

Bond Lengths (Å) for HL		Bond Angles (°) for HL	
O1-C2	1.445(2)	C3-O1-C2	116.8(2)
O1-C3	1.343(2)	O1-C2-C1	107.4(2)
O2C3	1.210(2)	O1-C3-C4	112.4(2)
O3-C12	1.349(2)	O2-C3-O1	122.7(2)
O4-C14	1.363(2)	O2-C3-C4	124.9(2)
O4-C17	1.425(2)	C6-C7-N1	116.7(2)
N1-C7	1.411(2)	C8-C7-N1	125.0(2)
N1-C10	1.284(2)	C10-N1-C7	122.0(2)
C12-C13	1.386(2)	N1-C10-C11	122.3(2)
C13-C14	1.382(2)	O3-C12-C11	121.1(2)
		O3-C12-C13	118.3(2)
		O4-C14-C13	124.7(2)
		O4-C14-C15	114.5(2)
		C14-O4-C17	117.6(2)

Table 2. Selected bond lengths (Å) and bond angles (°) for compound 6.

Bond Lengths (Å) for 6			
Cu1-S1	2.406(2)	C11-O17	1.363(7)
Cu1-O9	1.952(4)	C11-O20	1.374(6)
Cu1-O5	1.941(4)	C11-O18	1.375(7)
Cu1-O1	2.244(4)	C11-O19	1.42(1)
Cu1-N3	1.957(5)	O5-C23	1.324(7)
Cu2-S2	2.404(2)	C6-O1	1.282(7)
Cu2-O9	1.947(4)	N2-C25	1.317(8)
Cu2-O5	1.965(4)	N2-C26	1.409(8)
Cu2-N2	1.956(5)	N3-C43	1.423(9)
Cu2-O13	2.323(4)	O13-C57	1.292(7)
Cu2-O1 _w	2.356(6)	S1-C7	1.769(6)
S2-C41	1.786(6)	S1-C24	1.788(6)
S2-C58	1.777(6)	O9-C40	1.320(7)
Bond Angles (°) for 6			
O9-Cu1-S1	161.5(1)	O5-Cu2-O1W	92.1(2)
O9-Cu1-O1	99.5(2)	N2-Cu2-S2	105.4(2)
O9-Cu1-N3	92.1(2)	N2-Cu2-O5	92.4(2)
O5-Cu1-S1	84.1(1)	N2-Cu2-O13	87.9(2)
O5-Cu1-O9	77.6(2)	N2-Cu2-O1W	95.9(2)
O5-Cu1-O1	91.9(2)	O13-Cu2-S2	76.8(1)
O5-Cu1-N3	169.7(2)	O13-Cu2-O1W	169.4(2)
O1-Cu1-S1	78.1(1)	O1W-Cu2-S2	92.6(2)
N3-Cu1-S1	106.1(2)	Cu2-O9-Cu1	101.9(2)
N3-Cu1-O1	88.8(2)	Cu1-O5-Cu2	101.7(2)
O9-Cu2-S2	84.6(1)	O17-C11-O20	108.8(5)
O9-Cu2-O5	77.2(2)	O17-C11-O18	113.2(6)
O9-Cu2-N2	168.8(2)	O17-C11-O19	104.4(8)
O9-Cu2-O13	89.4(2)	O20-C11-O18	114.7(4)
O9-Cu2-O1W	88.7(2)	O20-C11-O19	107.7(6)
O5-Cu2-S2	161.0(1)	O18-C11-O19	107.3(6)
O5-Cu2-O13	97.6(2)		

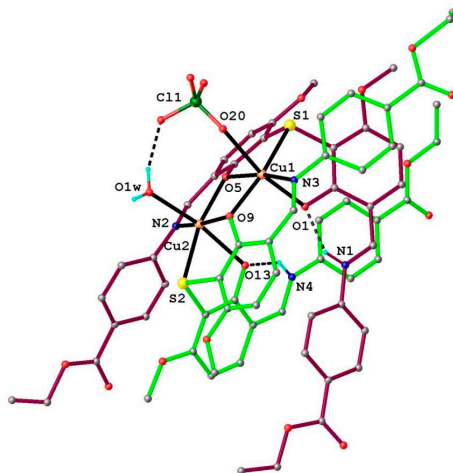


Figure 6. The X-ray structure of the complex cation $[\text{Cu}_2(\text{L}_2\text{S})_2(\text{ClO}_4)(\text{H}_2\text{O})]^+$ (**6**). H-bonds parameters: N1–H \cdots O1 [N1–H 0.86 Å, H \cdots O1 1.79 Å, N1 \cdots O1 2.526(7) Å, N1–H \cdots O1 141.7°]. N4–H \cdots O13 [N1–H 0.85 Å, H \cdots O13 1.80 Å, N4 \cdots O13 2.522(7) Å, N4–H \cdots O13 140.0°]. O1_w–H \cdots O19 [N1–H 0.85 Å, H \cdots O19 1.93 Å, O1_w \cdots O19 2.74(1) Å, O1_w–H \cdots O19 161.3°].

In the complex cation two Cu^{2+} ions, separated by 3.029(1) Å, are coordinated by two mono-deprotonated HL^- ligands, so that the charge balance is in agreement with the formation of species $[\text{Cu}_2(\text{L}_2\text{S})_2\text{ClO}_4\text{H}_2\text{O}]^+$. The separate structure of the coordinated ligands along with the atomic labeling scheme is presented in Figure 7a,b. Both the ligands are identical from the chemical point of view and exhibit very close geometric parameters (Table 2). The localization of the hydrogen atoms using the difference density Fourier map has clearly shown that the non-coordinated azomethine atoms N1 and N4 are the sites of protonation associated with the hydrogen bonding towards phenolic oxygen atoms as acceptor (Figures 6 and 7). The copper atoms adopt a slightly distorted octahedral $[\text{O}_4\text{NS}]$ coordination completed by ClO_4^- anion and H_2O molecule as monodentate ligands for Cu1 and Cu2, respectively (Figure 8).

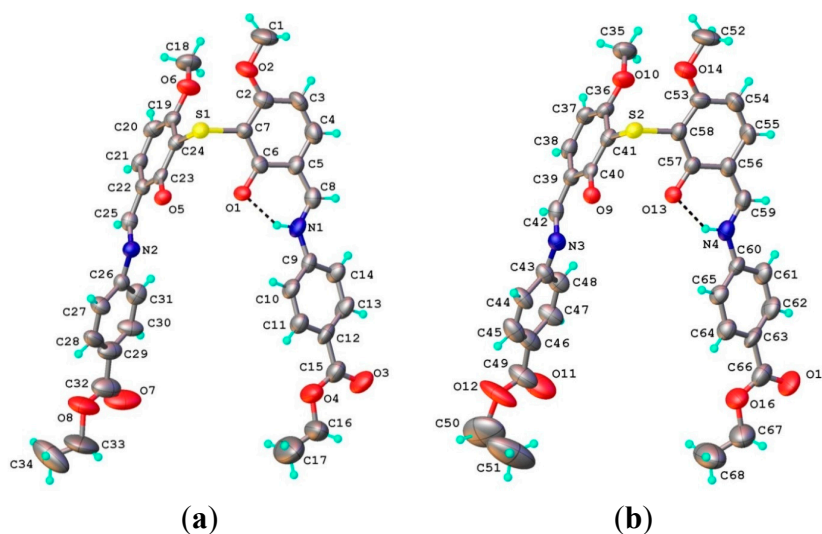


Figure 7. Structure of the two ligands (L_2S) in the complex cation $[\text{Cu}_2(\text{L}_2\text{S})_2(\text{ClO}_4)(\text{H}_2\text{O})]^+$.

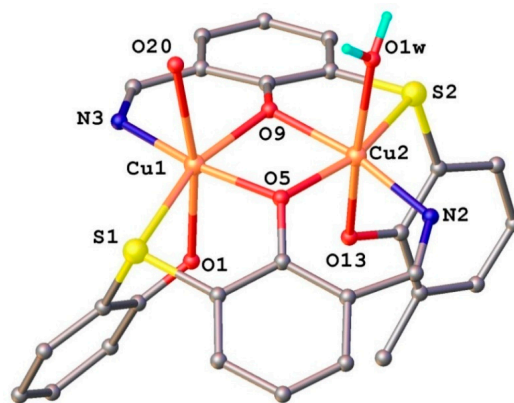


Figure 8. The coordination mode for the copper atoms of in the binuclear complex $[\text{Cu}_2(\text{L}_2\text{S})_2(\text{ClO}_4)(\text{H}_2\text{O})]^+$.

The crystal structure of complex **6** is characterized by the parallel packing of two dimensional supramolecular layers consolidated due to the numerous O-H \cdots O and C-H \cdots O hydrogen bonding, as shown in Figure 9.

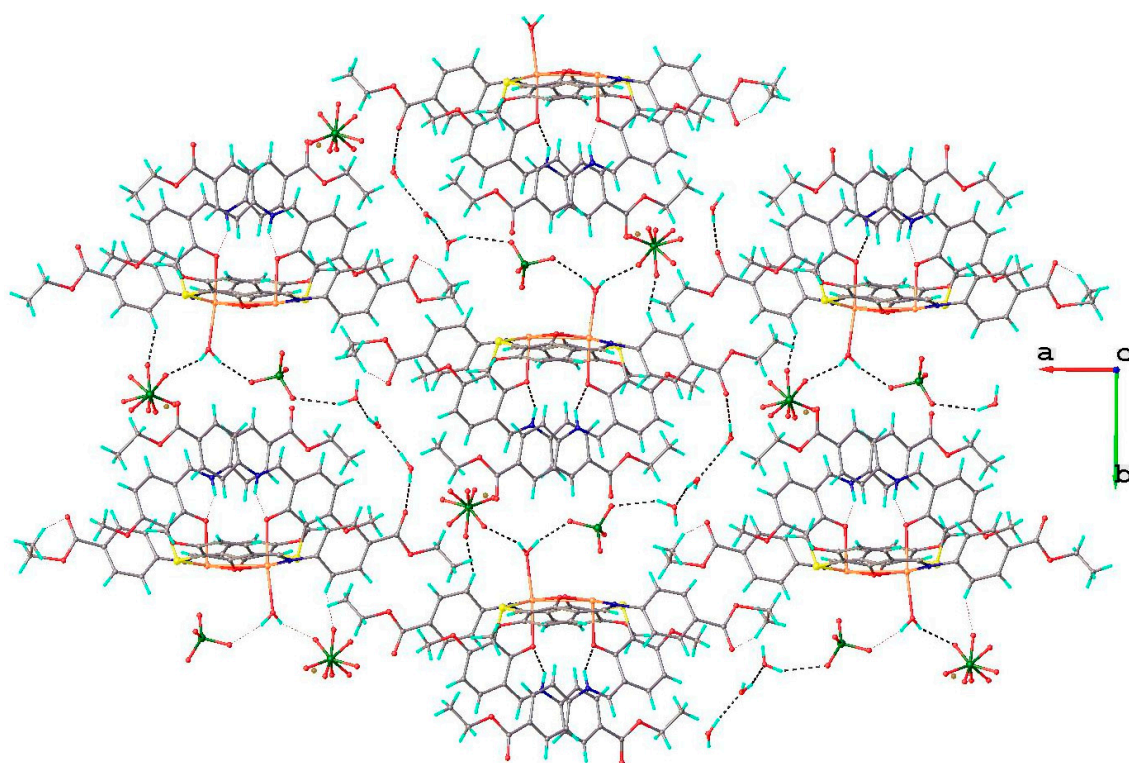


Figure 9. View of 2D supramolecular layer in the crystal structure **6**.

2.1.3. Infrared Spectra and Coordination Mode

The ligand and complexes have been characterized in detail by recording their IR spectra. The proposed assignments are based on previous results [28–31] and pertinent bibliography [32–35]. The $\nu(\text{C}=\text{N})$ band of the ligand at 1622 cm^{-1} is found to be shifted to lower energies ($1603\text{--}1595\text{ cm}^{-1}$) in the spectra of the complexes, indicating coordination via the azomethine nitrogen. The phenolic $\nu(\text{C}-\text{O})$ stretching vibration in the free Schiff base is observed at 1113 cm^{-1} , which is shifted by

10–21 cm^{-1} towards lower wave numbers in the complexes, thus indicating coordination of the phenolic oxygen to the Cu^{2+} ion [36].

In the IR spectra of complexes **1**, **4** and **5**, a considerable peak observed in the 3467–3420 cm^{-1} range supports the presence of $\nu(\text{H}_2\text{O})$ in the complexes [37]. The nitrate complex **1** has two bands at 1433 and 1182 cm^{-1} corresponding to ν_5 and ν_1 , with a separation of 250 cm^{-1} , and a medium band at 930 cm^{-1} assigned to ν_2 of the nitrate group, values that indicate bidentate coordination [38,39].

The acetate complex **3** has two strong bands at 1530 and 1442 cm^{-1} corresponding to $\nu_{\text{as}}(\text{COO}^-)$ and $\nu_{\text{s}}(\text{COO}^-)$ with a difference between frequencies of 88 cm^{-1} . This difference confirms the bidentate nature of the coordinated acetate [40].

The perchlorate complex **5** shows a band at 1108 cm^{-1} assignable to $\nu_3(\text{ClO}_4^-)$ and a strong band at 1090 cm^{-1} assignable to $\nu_4(\text{ClO}_4^-)$. The splitting of this band in two components indicates the presence of a monodentate perchlorate group [33,38].

2.1.4. Electronic Spectra and Magnetic Studies

The tentative assignments of the significant electronic spectral bands of ligand and of complexes are presented in Table 3. In these spectra, there is an intense band at 33,330 cm^{-1} which is assigned to a $\pi \rightarrow \pi^*$ transition originating in the phenyl ring [41]. The band at 28,570 cm^{-1} is attributed to an $n \rightarrow \pi^*$ transitions originating in the $-\text{CH}=\text{N}-$ chromophore [42]. In the spectra of the complexes these bands are shifted to lower energies (Figure S2).

Table 3. Electronic spectra (cm^{-1}) and magnetic moments (BM) of the complexes **1–5**.

Metal Complex	Transitions d–d (cm^{-1})			μ_{eff} (BM)	Geometry
[Cu(L)(NO ₃)(H ₂ O) ₂] (1)	${}^2\text{B}_{1g} \rightarrow {}^2\text{A}_{1g}$ 10,500	${}^2\text{B}_{1g} \rightarrow {}^2\text{B}_{2g}$ 13,420	${}^2\text{B}_{1g} \rightarrow {}^2\text{E}_g$ 19,400	1.98	Octahedral distorted
[Cu(L) ₂] (2)	${}^2\text{B}_2 \rightarrow {}^2\text{E}$ 11,100	${}^2\text{B}_2 \rightarrow {}^2\text{B}_1({}^2\text{A}_1)$ 13,100	-	1.87	Pseudo-tetrahedral
[Cu(L)(OAc)] (3)	${}^2\text{B}_2 \rightarrow {}^2\text{E}$ 10,980	${}^2\text{B}_2 \rightarrow {}^2\text{B}_1({}^2\text{A}_1)$ 13,500	-	1.92	Pseudo-tetrahedral
[Cu ₂ (L) ₂ Cl ₂ (H ₂ O) ₄] (4)	${}^2\text{B}_{1g} \rightarrow {}^2\text{A}_{1g}$ 11,000	${}^2\text{B}_{1g} \rightarrow {}^2\text{B}_{2g}$ 12,820	${}^2\text{B}_{1g} \rightarrow {}^2\text{E}_g$ 16,940	1.07	Octahedral distorted
[Cu(L)(ClO ₄)(H ₂ O)] (5)	${}^2\text{B}_2 \rightarrow {}^2\text{E}$ 9850	${}^2\text{B}_2 \rightarrow {}^2\text{B}_1({}^2\text{A}_1)$ 12,200	-	1.90	Pseudo-tetrahedral

The electronic spectra for the Cu(II) complexes **2**, **3** and **5** exhibit two bands in the region 10,980–11,100 cm^{-1} respectively 13,150–13,880 cm^{-1} , attributed to transitions d–d: ${}^2\text{B}_2 \rightarrow {}^2\text{E}$, ${}^2\text{B}_2 \rightarrow {}^2\text{B}_1({}^2\text{A}_1)$, suggesting a distorted tetrahedral geometry [43,44]. The values of the magnetic momentum (1.87, 1.92 and 1.90 BM) indicate the existence of copper complexes under monomers form. The spectrum for complex **1** exhibit three bands at 10,500, 13,420 and 19,410 cm^{-1} corresponding to the transitions: ${}^2\text{B}_{1g} \rightarrow {}^2\text{A}_{1g}$, ${}^2\text{B}_{1g} \rightarrow {}^2\text{B}_{2g}$, ${}^2\text{B}_{1g} \rightarrow {}^2\text{E}_g$, specific to the octahedral complexes with $d_{x^2-y^2}$ ground state [43].

The magnetic moment value 1.98 BM for complex **1** indicative of a non-bridging copper(II) complex. The electronic spectrum of complex **4** exhibit three bands at 11,000, 12,110 and 16,940 cm^{-1} corresponding to the transitions: ${}^2\text{B}_{1g} \rightarrow {}^2\text{A}_{1g}$, ${}^2\text{B}_{1g} \rightarrow {}^2\text{B}_{2g}$, ${}^2\text{B}_{1g} \rightarrow {}^2\text{E}_g$ suggesting an octahedral geometry [43].

The magnetic moment of the complex **4**, measured at room temperature, is 1.07 BM, per copper center. The subnormal magnetic moment indicates that the copper centers are anti-ferromagnetically coupled [45–54].

2.1.5. Mass Spectra

The FAB mass spectra of Cu(II) complexes with base Schiff **HL** have been recorded (Table S1). The mass spectrum of ligand showing a peak at $m/z = 300.12$ corresponds to the molecular ion $[M]^+$ (Figure S3).

$[M]^+$ peak obtained from the complexes are as follow: $m/z = 386.9$ (**1**), $m/z = 658.0$ (**2**), $m/z = 399.1$ (**3**), $m/z = 759.0$ (**4**), $m/z = 361.0$ (**5**). The results of mass spectrometry are consistent with the proposed formulas for these compounds as the peaks observed in these spectra correspond to fragments resulting from the expected fragmentations of the compounds.

2.1.6. EPR Spectra

The EPR spectra of the complexes in the polycrystalline state at 298 K and 77 K, were recorded at X-band, using 100 kHz field modulation. The g factors were quoted relative to the standard marker TCNE. The spectra of the compounds **1** and **4** in the polycrystalline state (293 K) show typical axial behavior with different g_{\parallel} and g_{\perp} values (Table 4). The geometric parameter G which is a measure of the exchange interaction between the copper centers in the polycrystalline compound is calculated using the equation: $G = (g_{\parallel} - 2.0023)/(g_{\perp} - 2.0023)$, for axial spectra [55]. In the copper(II) complexes **1** and **4**, $g_{\parallel} > g_{\perp} > 2.0023$ and G values (2.77, 3.99) are consistent with a $d_{x^2-y^2}$ ground state [56]. The spectra of compounds **2**, **3** and **5** show only one broad signal at 2.097, 2.102 and 2.127, respectively, (Figure 10) consistent with tetrahedral geometry [57].

Table 4. EPR spectral parameters of the copper(II) complexes **1–5**.

	1	2	3	4	5
Polycrystalline (298K)					
g_{\parallel}	2.230	-	-	2.132	-
g_{\perp}	2.060	-	-	2.059	-
g_{iso}	-	2.097	2.102	-	2.127
DMSO (77 K)					
g_{\parallel}	2.400	2.290	2.289	2.239	2.282
g_{\perp}	2.078	2.075	2.065	2.055	2.060
A_{\parallel}	117.0	162.0	150.2	170.0	170.0
α^2	0.802	0.800	0.779	0.772	0.817
β^2	0.997	0.948	0.990	0.990	0.887
δ^2	0.862	0.958	0.922	0.950	0.801
K_{\parallel}	0.800	0.755	0.762	0.770	0.718
K_{\perp}	0.692	0.760	0.715	0.735	0.658

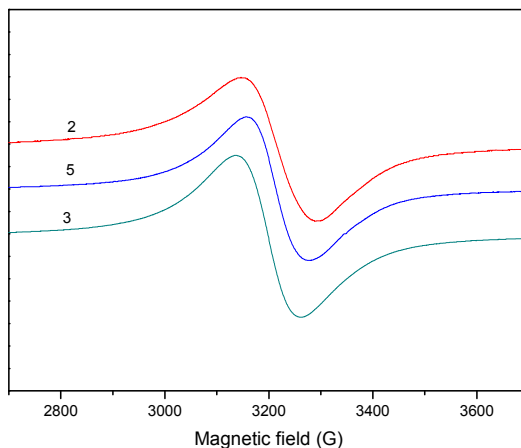


Figure 10. EPR spectra for the complexes **2**, **3** and **5** in powder, at room temperature.

The solution of complexes were recorded in DMSO at 298 K and 77 K. They present well-resolved four hyperfine lines (Figure 11).

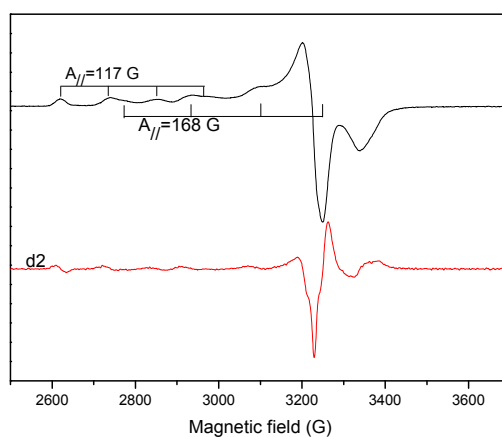


Figure 11. EPR spectrum of the complex **1**, in DMSO solution, registered at 77 K and (d2) second derivative spectra.

Spectra of the complexes **1**, **3** and **5** show three nitrogen superhyperfine lines in the perpendicular component (Figure 12).

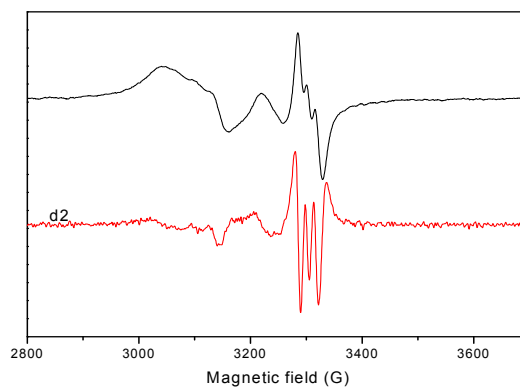


Figure 12. EPR spectrum (the derived signal) for complex **5** in DMSO solution at 77.

The binuclear nature of **4** was confirmed by the presence of half-field signals at *ca.*1600 G (Figure 13).

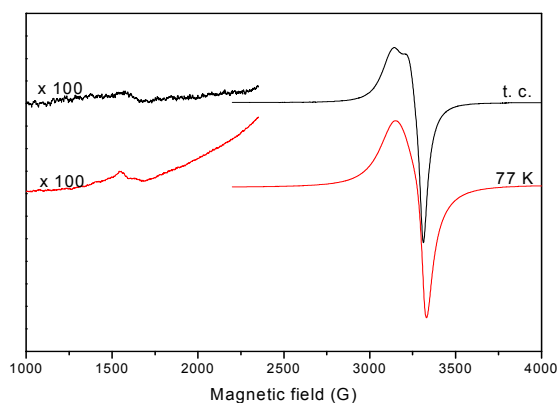


Figure 13. EPR spectrum of the complex **4**, in solution, at room temperature and 77 K.

EPR spectral assignments of the copper (II) complexes and orbital reduction parameters are shown in Table 4. The EPR parameters g_{\parallel} , g_{\perp} , A_{\parallel} (Cu) and the energies of the d–d transition were used to evaluate the bonding parameters α^2 , β^2 and δ^2 , which may be regarded as measures of the covalency of the in-plane σ bonds, in-plane π bonds and out-of-plane π bonds [58,59]. The orbital reduction factors $K_{\parallel} = \alpha^2\beta^2$ and $K_{\perp} = \alpha^2\delta^2$, were calculated using expressions reported elsewhere [60]. Hathaway has pointed out that for pure σ bonding, $K_{\parallel} \sim K_{\perp} \sim 0.77$ and for in-plane π -bonding, $K_{\parallel} < K_{\perp}$, while for out-of-plane π -bonding, $K_{\parallel} > K_{\perp}$ [61].

2.2. Biological Activity

The synthesized compounds and ligand were tested for their *in vitro* antibacterial and antifungal activity against *Escherichia coli* ATCC 25922, *Salmonella enteritidis*, *Staphylococcus aureus* ATCC 25923, *Enterococcus* and *Candida albicans* strains using the paper disc diffusion method [62] (for the qualitative determination) and the serial dilutions in liquid broth method [63] for determination of MIC values. Furaciline and nistatine were used as reference substances.

Data from Table 5 confirm the fact that both the ligand **HL** and the coordinative complexes of copper have a reduced bacteriostatic activity within the limits of concentrations 0.5–10.0 mg/mL toward the gram-positive and gram-negative bacteria. A more nuanced sensitivity toward the searched complexes has been proved by the gram-positive micro-organisms. The experimental data obtained demonstrate that the bacteriostatic activity of the coordinative complexes is influenced by the number of ligand molecules **HL** found out in the inner sphere and ligand nature. Therefore, growing of the number of ligand molecules and replacing the ions chloro- or acetate- with the perchlorate ion leads to a growing of the antimicrobial activity. The complexes $[\text{Cu}(\text{L})_2]$ (**2**), $[\text{Cu}(\text{L})(\text{ClO}_4)(\text{H}_2\text{O})]$ (**5**) and $[\text{Cu}_2(\text{L}_2\text{S})(\text{ClO}_4)(\text{H}_2\text{O})]\text{ClO}_4 \cdot \text{H}_2\text{O}$ (**6**) develop bacteriostatic activity also toward *Candida albicans* in the area of concentrations 0.5–0.12 mg/mL, while the initial Schiff base **HL** which enters the inner sphere of these complexes doesn't develop antifungal activity.

Table 5. Antibacterial activities of ligand **HL** and complexes **1–5** as MIC ^a/MBC ^b values (mg/mL).

Compounds	<i>E. coli</i> (G ⁻)		<i>S. enteritidis</i> (G ⁻)		<i>S. aureus</i> (G ⁺)		<i>Enterococcus</i> (G ⁺)		<i>C. albicans</i>	
	MIC	MBC	MIC	MBC	MIC	MBC	MIC	MBC	MIC	MBC
C ₁₇ H ₁₇ NO ₄ (HL ⁴)	>10.0	>10.0	>10.0	>10.0	>10.0	>10.0	>10.0	>10.0	>10.0	>10.0
[Cu(L)(NO ₃)(H ₂ O) ₂] (1)	>10.0	>10.0	>10.0	>10.0	0.5	>10.0	0.5	>10.0	0.5	>10.0
[Cu(L) ₂] (2)	>10.0	>10.0	>10.0	>10.0	0.5	>10.0	0.5	>10.0	0.12	>10.0
[Cu(L)(OAc)] (3)	>10.0	>10.0	>10.0	>10.0	>10.0	>10.0	0.5	>10.0	>10.0	>10.0
[Cu ₂ (L) ₂ Cl ₂ (H ₂ O) ₄] (4)	>10.0	>10.0	>10.0	>10.0	0.5	>10.0	>10.0	>10.0	>10.0	>10.0
[Cu(L)(ClO ₄)(H ₂ O)] (5)	0.5	>10.0	>10.0	>10.0	0.5	>10.0	0.5	>10.0	0.12	>10.0
Furacillinum	0.018	0.037	0.009	0.009	0.009	0.009	0.037	0.037	-	-
Nystatine	-	-	-	-	-	-	-	-	0.08	0.08

E. coli (Escherichia coli, ATCC 25922); *S. enteritidis* (Salmonella enteritidis); *S. aureus* (Staphylococcus aureus, ATCC 25923); *C. albicans* (Candida albicans); ^a MIC—Minimum inhibitory concentration;

^b MBC—Minimum bactericide concentration; G(-): Gram-negative bacteria; G(+): Gram-positive bacteria.

3. Experimental

3.1. General Information

All commercially available reagents and chemicals were of analytical- or reagent-grade purity and used as received. The chemical elemental analysis for the determination of C, H, N was done on a Carlo-Erba LA-118 microdosimeter (Lakewood, CA, USA). ¹H-NMR and ¹³C-NMR spectra were recorded at room temperature on a Bruker DRX 400 spectrometer (Billerica, MA, USA) in DMSO-d₆, using TMS as the internal standard. IR spectra were recorded on a Specord-M80 spectrophotometer (Leipzig, Germany) in the 4000–400 cm⁻¹ region using KBr pellets. The complexes were studied by thermogravimetry (TG) in a static air atmosphere, with a sample heating rate of 10 °C/min using a STA 6000 Perkin Elmer (Waltham, MA, USA). Electronic spectra were recorded using the JascoV-670 spectrophotometer (Tokyo, Japan) in diffuse reflectance, using MgO dilution matrices. EPR spectra were recorded on polycrystalline powders and DMSO solutions at room temperature and 77 K with an MiniScope MS200, (Magnettech Ltd., Berlin, Germany), X-band spectrometer (9.3–9.6 GHz), connected to a PC equipped with a 100 KHz field modulation unit. High resolution mass spectra were recorded on a ThermoScientific (LTQ XLOrbitrap) spectrometer using APCI ionization technique and Orbital Ion Trap mass analyzer (Rockford, IL, USA).

The molar conductance of the complexes in *N,N'*-dimethylformamide solutions (10⁻³ M), at room temperature, were measured using a Consort type C-533 conductivity instrument. The magnetic susceptibility measurements were done at room temperature in the polycrystalline state on a Faraday magnetic balance (home made).

Crystallographic measurements were carried out on Oxford-Diffraction XCALIBUR E CCD diffractometer (Santa Clara, CA, USA) equipped with graphite-monochromated MoK α radiation. The single crystals were positioned at 40 mm from the detector and 197 and 273 frames were measured each for 20 and 30 s over 1° scan width for **HL** and **6**, respectively. The unit cell determination and data integration were carried out using the CrysAlis package of Oxford Diffraction [64]. Both

structures were solved by direct methods using Olex2 [65] software with the SHELXS structure solution program and refined by full-matrix least-squares on F^2 with SHELXL-97 [66]. Atomic displacements for non-hydrogen atoms were refined using an anisotropic model. H atoms were placed at calculated positions and refined as riding atoms in the subsequent least-squares model refinements. The positional parameters of OH and NH hydrogen atoms were found from difference. The oxygen atoms in non-coordinated perchlorate anion were found to be severely disordered and their positional parameters were refined isotopically in combination with PART and SADI tools available in SHELXL. Crystallographic data together with refinement details are summarized in Table 6.

Table 6. Crystallographic data, details of data collection and structure refinement parameters for **HL** and **6**.

Compound	HL	6
Empirical formula	C ₁₇ H ₁₇ NO ₄	C ₆₈ H ₆₆ Cl ₂ Cu ₂ N ₄ O ₂₆ S ₂
Formula weight	299.32	1617.35
Temperature/K	200	293
Crystal system	monoclinic	monoclinic
Space group	<i>C2/c</i>	<i>P2₁/c</i>
<i>a</i> /Å	15.4089(7)	16.7582(11)
<i>b</i> /Å	6.4308(3)	26.2186(13)
<i>c</i> /Å	29.8710(16)	17.9269(12)
α /°	90.00	90.00
β /°	95.916(4)	107.710(8)
γ /°	90.00	90.00
<i>V</i> /Å ³	2944.2(2)	7503.4(8)
<i>Z</i>	8	4
<i>D</i> _{calc} /mg/mm ³	1.351	1.432
μ /mm ⁻¹	0.097	0.774
Crystal size/mm ³	0.2 × 0.1 × 0.1	0.35 × 0.35 × 0.1
θ_{\min} , θ_{\max} (°)	6.22 to 49.42	3.92 to 46.52
Reflections collected	4619	30514
Independent reflections	2404 [<i>R</i> _{int} = 0.0212]	10,753 [<i>R</i> _{int} = 0.0590]
Data/restraints/parameters	2404/0/201	10,753/29/942
GOF ^c	1.010	1.028
<i>R</i> ₁ ^a (<i>I</i> > 2σ(<i>I</i>))	0.0434	0.0791
<i>wR</i> ₂ ^b (all data)	0.1020	0.2287
Largest diff. peak/hole/e Å ⁻³	0.11/−0.15	0.72/−0.87

^a $R_1 = \Sigma||F_o| - |F_c||/\Sigma|F_o|$; ^b $wR_2 = \{\Sigma[w(F_o^2 - F_c^2)^2] / \Sigma[w(F_o^2)^2]\}^{1/2}$; ^c $GOF = \{\Sigma[w(F_o^2 - F_c^2)^2] / (n - p)\}^{1/2}$, where *n* is the number of reflections and *p* is the total number of parameters refined.

3.2. Chemistry

3.2.1. Synthesis of the Schiff Base Ethyl 4-[(E)-(2-hydroxy-4-methoxyphenyl)methyleneamino] benzoate (**HL**)

A solution of 2-hydroxy-4-methoxybenzaldehyde (0.152 g, 1 mmol) in ethanol (10 mL) was added to a solution of ethyl-4-aminobenzoate (0.165 g, 1 mmol) in ethanol (20 mL). The mixture was stirred for 1 h at 25 °C, then refluxed for 4 h and kept at 4 °C for several days. The characteristic yellow precipitate obtained by Schiff base condensation was filtered out and kept for crystallization. Fine yellow crystals obtained upon slow evaporation at room temperature were characterized, including single crystal X-ray diffraction. Yield 81%. M.p. 125–127 °C. Anal. Calc. for C₁₇H₁₇NO₄: C, 68.15; H, 5.67; N, 4.67. Found: C, 68.42; H, 5.43; N, 4.41%. The IR spectrum of the obtained ligand confirms the occurrence of the absorption band of 1622 cm⁻¹ (st, intense), specific for the azomethinic group [39]. The ¹H NMR spectra (CDCl₃, d, ppm, J, Hz), recorded in CDCl₃, for the ligand has the following signals confirming the structure of the ligand: ¹H-NMR (CDCl₃, δ, ppm, J, Hz): 1.40 (s, 3H, CH₃); 3.84 (s, 3H, OCH₃); 4.40 (s, 2H, CH₂); 6.13 (d, 8.5, 1H, H-13); 6.50 (d, 8.5, 1H, H-15); 7.26 (s 1H, H-16); 7.60–8.15 (m, 4H, benzene); 8.53 (s, 1H, CH=N). ¹³C-NMR (CDCl₃, δ, ppm): 14.48 (CH₃); 55.63 (O-CH₃); 61.13(OCH₂); 101.19 (C-13); 107.67 (C-15); 113.07 (C-11); 121.06 (C-8); 128.30 (C-4); 131.10 (C-5); 134.06 (C-9); 152.52 (C-N=CH); 162.90 (C-OH); 164.20 (C=N); 164.63 (C-OCH₃); 166.30 (C=O). The ligand is soluble in chloroform and dichloromethane.

3.2.2. General Procedure for the Preparation of the Metal Complexes 1–6

Complexes **1–5** were prepared by direct reaction between the ligand and the corresponding metal salts. Complex **6** was obtained by stirring a mixture of ligand, Cu(ClO₄)₂·6H₂O and NaSCN.

Synthesis of the complex [Cu(L)(NO₃)(H₂O)₂] (1): A methanol solution (15 mL) of the ligand HL (0.299 g, 1 mmol) was added to Cu(NO₃)₂·3H₂O (0.241g, 1 mmol) dissolved in methanol (10 mL). The resulting solution was stirring for 6 h at 50 °C. The green colored solid was filtered, washed with methanol, diethylether and then dried *in vacuo*. Anal. Calc. for C₁₇H₂₀CuN₂O₉: C, 44.39; H, 4.35; N, 6.09; Cu, 13.81. Found: C, 44.60; H, 4.12; N, 5.88; Cu, 13.62%. M.wt.: 459.5; M.p. > 250 °C; Yield: 82%; Main IR peaks (KBr, cm⁻¹): ν(OH) 3420; ν(C=O) 1705; ν (C=N) 1595; ν(Ar–OH) 1100; ν(Ar–O–C_{aliphatic}) 1274, 1025; ν₅(NO₃⁻) 1433; ν₁(NO₃⁻) 1182.

Synthesis of the complex [Cu(L)₂] (2): Complex **2** was prepared similarly, using CuSO₄·5H₂O (1 mmol). Brown solid. Anal. Calc. for C₃₄H₃₂CuN₂O₈: C, 61.86; H, 4.85; N, 4.24; Cu, 9.62. Found: C, 62.04; H, 4.52; N, 4.01; Cu, 9.38%. M.wt.: 659.5; M.p. > 250 °C; Yield: 87%; Main IR peaks (KBr, cm⁻¹): ν(C=O) 1706; ν(C=N) 1603; ν(Ar–OH) 1092; ν(Ar–O–C_{aliphatic}) 1272, 1023.

Synthesis of the complex [Cu(L)(OAc)] (3): Complex **3** was prepared similarly, using Cu₂(OAc)₄·(H₂O)₂ (1 mmol). Brown solid. Anal. Calc. for C₁₉H₁₉CuNO₆: C, 54.22; H, 4.51; N, 3.32; Cu, 15.10. Found: C, 54.63; H, 4.24; N, 3.08; Cu, 14.87%. M.wt.: 420.5; M.p. > 250 °C; Yield: 76%; Main IR peaks (KBr, cm⁻¹): ν(C=O) 1703; ν(C=N) 1602; ν(Ar–OH) 1103; ν(Ar–O–C_{aliphatic}) 1277, 1025; ν_{as}(COO⁻)1530; ν_s(COO⁻) 1442.

Synthesis of the complex [Cu₂(L)₂Cl₂(H₂O)₄] (4): Complex **4** was prepared similarly, using CuCl₂·2H₂O (1 mmol). Light brown solid. Anal. Calc. for C₃₄H₄₀Cu₂N₂O₁₂Cl₂: C, 47.11; H, 4.61; N, 3.23; Cu, 14.66. Found: C, 46.83; H, 4.30; N, 3.02; Cu, 14.38%. M.wt.: 866; M.p. > 250 °C; Yield: 81%; Main IR peaks (KBr, cm⁻¹): ν(OH) 3440; ν(C=O) 1702; ν(C=N) 1601; ν(Ar-OH) 1101; ν(Ar-O-C_{aliphatic}) 1273, 1024.

Synthesis of the complex [Cu(L)(ClO₄)(H₂O)] (5): Complex **5** was prepared similarly, using Cu(ClO₄)₂·6H₂O (1 mmol). Brown solid. Anal. Calc. for C₁₇H₁₈CuNO₉Cl: C, 42.58; H, 3.75; N, 2.92; Cu, 13.25. Found: C, 42.24; H, 3.52; N, 2.68; Cu, 13.03%. M.wt.: 479; M.p. > 250 °C; Yield: 79%; Main IR peaks (KBr, cm⁻¹): ν(OH) 3467; ν(C=O) 1706; ν(C=N) 1599; ν(Ar-OH) 1093; ν(Ar-O-C_{aliphatic}) 1276, 1021; ν₃(ClO₄⁻) 1108; ν₄(ClO₄⁻) 1090.

Synthesis of the complex [Cu₂(H₂L₂S)(ClO₄)(H₂O)]ClO₄·H₂O (6): A solution of 2-hydroxy-4-methoxybenzaldehyde (0.152 g, 1 mmol) in methanol (10 mL) was added to a solution of ethyl-4-aminobenzoate (0.165 g, 1 mmol) in methanol (20 mL). The reaction mixture was refluxed for 3 h. Copper(II) perchlorate hexahydrate (0.340 g, 1 mmol) dissolved in methanol was added and the mixture was refluxed for 1 h. Finally 5 mL methanolic solution of NaSCN (0.162 g, 2 mmol) was added dropwise, the mixture was refluxed for another 1 h and the resulting solution was then filtered. Reddish brown single crystals suitable for structure determination were obtained from methanolic solution within few days. Anal. Calc. for C₆₈H₆₆Cl₂Cu₂N₄O₂₆S₂: C, 50.46; H, 4.08; N, 3.46; Cu, 7.91. Found: C, 50.86; H, 3.82; N, 3.24; Cu, 7.82%. M.wt.: 1617; M.p. > 250 °C; Yield: 83%; Main IR peaks (KBr, cm⁻¹): ν(OH) 3450; ν(C=O) 1702; ν(C=N) 1596; ν(Ar-OH) 1095; ν(Ar-O-C_{aliphatic}) 1272, 1025; ν₃(ClO₄⁻) 1106; ν₄(ClO₄⁻) 1090.

3.3. Antibacterial Activity

The antibacterial activity of complexes and also of their prototype furaciline has been determined under liquid nutritive environment [2% of peptone bullion (pH 7.0)] using successive dilutions method [67–69]. *Escherichia coli*, *Salmonella enteritidis*, *Staphylococcus aureus*, *Enterococcus* stems were used as reference culture for *in vitro* experiment. The dissolution of studied substances in dimethylformamide, microorganisms cultivation, suspension obtaining, determination of minimal inhibition concentration (MIC) and minimal bactericide concentration (MBC) have been carried out according to the method previously reported.

3.4. Antifungal Bioassay

Antimycotic properties of the complexes were investigated *in vitro* on laboratory stem *Candida albicans*. The activity has been determined in liquid Sabouroud nutritive environment (pH 6.8). The inoculates were prepared from fungal stems which were harvested from 3–7 day-old cultures. Their concentration in suspension was (2–4) × 10⁶ colony forming units per milliliter. Sowings for fungi and micelles were incubated at 37 °C during 7 and 14 days, respectively.

4. Conclusions

The analytical and physico-chemical analyses confirm the composition and the structure of the newly obtained complex combinations. In all the complexes, the ligand base Schiff, **HL** acts as mono-negative bidentate around the metal ion. The structure of the ligand **HL** and complex **6** has been determined by single-crystal X-ray diffraction. This fact indicates for complex **6** a bi-nuclear system where every atom of Cu(II) is hexacoordinated through the medium of 4 atoms of oxygen, one atom of nitrogen and one atom of sulfur. The two atoms of copper (II) are united each other through the medium of two atoms of oxygen coming from the hydroxyl groups grafted on the aldehyde nucleus.

The EPR parameters g_{\parallel} , g_{\perp} , A_{\parallel} and the energies of d–d transitions were used to evaluate the bonding parameters. The orbital reduction factors indicate the presence of out-of-plane π -bonding for complexes **1**, **3–5** and of some in-plane π -bonding for the complex **2**.

The antimicrobial activity data obtained indicate that the activity of the metal complexes is higher than ligands. The structure of the compounds tested has an effect on antimicrobial activity.

Supplementary Materials

Supplementary materials can be accessed at: <http://www.mdpi.com/1420-3049/20/04/5771/s1>.

Acknowledgments

The authors thank the Organic Chemistry Department, ICECHIM Bucharest (Romania) for microanalysis, “Horia Hulubei” National Institute of Physics and Nuclear Engineering Bucharest for help with EPR spectroscopy. The authors wish to thank the State University of Medicine and Pharmacy of Chisinau (Moldova) for their help in carrying out biological studies. Supported by National Authority for Scientific Research of Ministry of Education and Research, Bucharest, Romania (Bilateral project with Republic of Moldova, No.680/2 2.04.2013).

Appendix

CCDC 1005531 and 1005532 contains the supplementary crystallographic data for $C_{17}H_{17}NO_4$ (**HL**) and $C_{68}H_{66}Cl_2Cu_2N_4O_{26}S_2$ (**6**). These data can be obtained free of charge via http://www.ccdc.cam.ac.uk/data_request/cif or from the Cambridge Crystallographic Data Centre, 12 Union Road, Cambridge CB2 1EZ, UK; Fax: +44-1223-336-033; or E-Mail: deposit@ccdc.cam.ac.uk.

Author Contributions

Elena Pahontu designed the research, performed the synthesis of the compounds, contributed to the analysis of the data and wrote the paper. Diana-Carolina Ilieş performed IR spectroscopy, thermal analysis and wrote the paper; Sergiu Shova performed X-ray diffraction studies; Codruța Paraschivescu performed FAB mass spectroscopy; Mihaela Badea performed UV-Vis spectroscopy; Aurelian Gulea performed antimicrobial activity; Tudor Roşu performed EPR spectroscopy and contributed to the interpretation of the data.

All authors read and approved the final manuscript.

Conflict of Interest

The authors declare no conflict of interest.

References

1. Rawal, R.K.; Tripathi, R.; Kati, S.B.; Pannecouque, C.; de Clercq, E. Design, synthesis, and evaluation of 2-aryl-3-heteroaryl-1,3-thiazolidin-4-ones as anti-HIV agents. *Bioorg. Med. Chem.* **2007**, *15*, 1725–1731.
2. Giovine, A.; Muraglia, M.; Florio, M.A.; Rosato, A.; Corbo, F.; Franchini, C.; Musio, B.; Degennaro, L.; Luisi, R. Synthesis of functionalized arylaziridines as potential antimicrobial agents. *Molecules* **2014**, *19*, 11505–11519.
3. Wang, P.H.; Keck, J.G.; Lien, E.J.; Lai, M.M.C. Design, synthesis, testing and quantitative structure-activity relationship analysis of substituted salicylaldehyde Schiff bases of 1-amino-3-hydroxyguanidine tosylate as new antiviral agents against coronavirus. *J. Med. Chem.* **1990**, *33*, 608–614.
4. Jarrahpour, A.; Motamedifar, M.; Pakshir, K.; Hadi, N.; Zarei, M. Synthesis of novel azo Schiff bases and their antibacterial and antifungal activities. *Molecules* **2004**, *9*, 815–824.
5. Omar, M.M.; Mohamed, G.G.; Ibrahim, A.A. Spectroscopic characterization of metal complexes of novel Schiff base. Synthesis, thermal and biological activity studies. *Spectrochim. Acta A* **2009**, *73*, 358–369.
6. Ceyhana, G.; Urus, S.; Demirtas, I.; Elmastas, M.; Tümer, M. Antioxidant, electrochemical, thermal, antimicrobial and alkane oxidation properties of tridentate Schiff base ligands and their metal complexes. *Spectrochim. Acta A* **2011**, *81*, 184–198.
7. Mladenova, R.; Ignatova, M.; Manolova, N.; Petrova, T.; Rashkov, I. Preparation, characterization and biological activity of Schiff base compounds derived from 8-hydroxyquinoline-2-carboxaldehyde and Jeffamines ED. *Eur. Polym. J.* **2002**, *38*, 989–999.
8. Huang, G.S.; Liang, Y.M.; Wu, X.L.; Liu, W.M.; Ma, Y.X. Some ferrocenyl Schiff bases with nonlinear optical properties. *Organomet. Chem.* **2003**, *17*, 706–710.
9. Walsh, O.M.; Meegan, M.J.; Prendergast, R.M.; Nakib, T.A. Synthesis of 3-acetoxyazetidines and 3-hydroxyazetidines with antifungal and antibacterial activity. *Eur. J. Med. Chem.* **1996**, *31*, 989–1000.
10. Liu, Y.; Yang, Z. Synthesis, crystal structure, antioxidation and DNA binding properties of binuclear Ho(III) complexes of Schiff-base ligands derived from 8-hydroxyquinoline-2-carboxaldehyde and four arylhydrazines. *J. Organomet. Chem.* **2009**, *694*, 3091–3101.
11. Santra, B.K.; Reddy, P.A.N.; Neelakanta, G.; Mahadevan, S.; Nethaji, M.; Chakravarty, A.R. Oxidative cleavage of DNA by a dipyrrodoquinoxaline copper(II) complex in the presence of ascorbic acid. *J. Inorg. Biochem.* **2002**, *89*, 191–196.
12. Aslantaş, M.; Kendi, E.; Demir, N.; Şabik, A.E.; Tümer, M.; Kertmen, M. Synthesis, spectroscopic, structural characterization, electrochemical and antimicrobial activity studies of the Schiff base ligand and its transition metal complexes. *Spectrochim. Acta A* **2009**, *74*, 617–624.

13. Chandra, S.; Kumar, A. Electronic, EPR and magnetic studies of Co(II), Ni(II) and Cu(II) complexes with thiosemicarbazone (L1) and semicarbazone (L2) derived from pyrole-2-carboxyaldehyde. *Spectrochim. Acta A* **2007**, *67*, 697–701.
14. Das, A.; Trousdale, M.D.; Ren, S.; Lien, E.J. Inhibition of herpes simplex virus type 1 and adenovirus type 5 by heterocyclic Schiff bases of aminohydroxyguanidine tosylate. *Antivir. Res.* **1999**, *44*, 201–208.
15. Shanker, K.; Rohini, R.; Reddy, P.M.; Ho, Y.P.; Ravinder, V. Ru(II) complexes of N₄ and N₂O₂ macrocyclic Schiff base ligands: Their antibacterial and antifungal studies. *Spectrochim. Acta A* **2009**, *73*, 205–211.
16. Kureshy, R.I.; Khan, N.H.; Abdi, S.H.R.; Patel, S.T.; Iyer, P. Chiral Ru(II) Schiff base complexes catalysed enantioselective epoxidation of styrene derivatives using iodosyl benzene as oxidant II. *J. Mol. Catal.* **1999**, *150*, 175–183.
17. Aoyama, Y.; Kujisawa, J.T.; Walanawe, T.; Toi, A.; Ogashi, H. Catalytic reactions of metalloporphyrins. 1. Catalytic modification of borane reduction of ketone with rhodium(III) porphyrin as catalyst. *J. Am. Chem. Soc.* **1986**, *108*, 943–947.
18. Kelly, T.R.; Whiting, A.; Chandrakumar, N.S. A rationally designed, chiral Lewis acid for the asymmetric induction of some Diels-Alder reactions. *J. Am. Chem. Soc.* **1986**, *108*, 3510–3512.
19. Sengupta, P.; Ghosh, S.; Mak, T.C.W. A new route for the synthesis of bis(pyridine dicarboxylato)bis(triphenylphosphine) complexes of ruthenium(II) and X-ray structural characterisation of the biologically active trans-[Ru(PPh₃)₂(L1H)₂] (L1H₂=pyridine 2,3-dicarboxylic acid). *Polyhedron* **2001**, *20*, 975–980.
20. Ibrahim, O.B.; Mohamed, M.A.; Refat, M.S. Nano Sized Schiff Base Complexes with Mn(II), Co(II), Cu(II), Ni(II) and Zn(II) Metals: Synthesis, Spectroscopic and Medicinal Studies. *Can. Chem. Trans.* **2014**, *2*, 108–121.
21. Green, D.R.; Reed, J.C. Mitochondria and apoptosis. *Science* **1998**, *281*, 1309–1312.
22. Easmon, J.; Pürstinger, G.; Heinisch, G.; Roth, T.; Fiebig, H.H.; Holzer, W.; Jäger, W.; Jenny, M.; Hofmann, J. Synthesis, cytotoxicity, and antitumor activity of copper(II) and iron(II) complexes of (4)N-azabicyclo[3.2.2]nonane thiosemicarbazones derived from acyl diazines. *J. Med. Chem.* **2001**, *44*, 2164–2171.
23. Kumar, S.; Dhar, D.N.; Saxena, P.N. Applications of metal complexes of Schiff bases—A review. *J. Sci. Ind. Res.* **2009**, *68*, 181–187.
24. Morrow, M.E.; Berry, C.W. Antimicrobial properties of topical anesthetic liquids containing lidocaine or benzocaine. *Anesth. Prog.* **1988**, *35*, 9–13.
25. Pongratz, Z. Über neue pharmakologisch wirksame Amide und Ester der Nicotinsäure. *Monatsh. Chem.* **1957**, *88*, 330–335.
26. Perrin, D.D.; Armarego, W.L.; Perrin, D.R. *Purification of Laboratory Chemicals*, 2nd ed.; Pergamon: New York, NY, USA, 1990; pp. 140–142.
27. Geary, W.J. The use of conductivity measurements in organic solvents for the characterization of coordination compounds. *Coord. Chem. Rev.* **1971**, *7*, 81–115.
28. Rosu, T.; Pahontu, E.; Maxim, C.; Georgescu, R.; Stanica, N.; Gulea, A. Some new Cu(II) complexes containing an ON donor Schiff base: Synthesis, characterization and antibacterial activity. *Polyhedron* **2011**, *30*, 154–162.

29. Rosu, T.; Pasculescu, S.; Lazar, V.; Chifiriuc, C.; Cernat, R. Copper(II) Complexes with Ligands Derived from 4-Amino-2,3-dimethyl-1-phenyl-3-pyrazoline-5-one. *Molecules* **2006**, *11*, 904–914.
30. Rosu, T.; Gulea, A.; Nicolae, A.; Georgescu, R. Complexes of 3d(n) metal ions with thiosemicarbazones: Synthesis and antimicrobial activity. *Molecules* **2007**, *12*, 782–796.
31. Rosu, T.; Negoiu, M.; Pasculescu, S.; Pahontu, E.; Poirier, D.; Gulea, A. Metal-based biologically active agents: Synthesis, characterization, antibacterial and antileukemia activity evaluation of Cu(II), V(IV) and Ni(II) complexes with antipyrine-derived compounds. *Eur. J. Med. Chem.* **2010**, *45*, 774–781.
32. Rosu, T.; Pahontu, E.; Maxim, C.; Georgescu, R.; Stanica, N.; Almajan, G.L.; Gulea, A. Synthesis, characterization and antibacterial activity of some new complexes of Cu(II), Ni(II), VO(II), Mn(II) with Schiff base derived from 4-amino-2,3-dimethyl-1-phenyl-3-pyrazolin-5-one. *Polyhedron* **2010**, *29*, 757–766.
33. Raphael, P.F.; Manoj, E.; Prathapachandra Kurup, M.R. Copper(II) complexes of N(4)-substituted thiosemicarbazones derived from pyridine-2-carbaldehyde: Crystal structure of a binuclear complex. *Polyhedron* **2007**, *26*, 818–828.
34. Khandar, A.A.; Hosseini-Yazdi, S.A. Synthesis, X-ray crystal structure, and solution properties of nickel(II) complexes of new 16-membered mixed-donor macrocyclic Schiff base ligand incorporating a pendant alcohol function. *Polyhedron* **2003**, *22*, 1481–1487.
35. Vicente, M.; Bastida, R.; Lodeiro, C.; Macias, A.; Parola, A.J.; Valencia, L.; Spey, S.E. Metal complexes with a new N₄O₃ amine pendant-armed macrocyclic ligand: Synthesis, characterization, crystal structures, and fluorescence studies. *Inorg. Chem.* **2003**, *42*, 6768–6779.
36. Lodeiro, C.; Bastida, R.; Bertolo, E.; Macias, A.; Rodriguez, A. Coordination chemistry of copper(II) with oxaza macrocyclic ligands: Crystal structure of a dinuclear tetramer copper(II) complex. *Polyhedron* **2003**, *22*, 1701–1710.
37. Kannappan, R.; Tanase, S.; Mutikainen, I.; Turpeinen, U.; Reedijk, J. Low-spin iron(III) Schiff-base complexes with symmetric hexadentate ligands: Synthesis, crystal structure, spectroscopic and magnetic properties. *Polyhedron* **2006**, *25*, 1646–1654.
38. Patel, R.N.; Gundla, V.L.N.; Patel, D.K. Synthesis, structure and properties of some copper(II) complexes containing an ONO donor Schiff base and substituted imidazole ligands. *Polyhedron* **2008**, *27*, 1054–1060.
39. Nakamoto, K. *Infrared Spectra of Inorganic and Coordination Compounds*; Wiley and Sons: New York, NY, USA, 1986; pp. 212, 232, 248, 251, 256.
40. Nakamoto, K. *Infrared and Raman Spectra of Inorganic and Coordination Compounds*, 5th ed.; Wiley-Interscience: New York, NY, USA, 1997; p. 86.
41. Belicchi-Ferrari, M.; Bisceglie, F.; Cavalieri, C.; Pelosi, G.; Tarasconi, P. Bis(triphenylphosphine)4-fluorobenzaldehyde thiosemicarbazone copper(I): Forcing chelation through oxoanions. *Polyhedron* **2007**, *26*, 3774–3782.
42. Bosnich, B. An interpretation of the circular dichroism and electronic spectra of salicylaldehyde complexes of square-coplanar diamagnetic nickel(II). *J. Am. Chem. Soc.* **1968**, *90*, 627–632.
43. Dowing, R.S.; Urbach, F.L. Circular dichroism of square-planar, tetradentate Schiff base chelates of copper(II). *J. Am. Chem. Soc.* **1969**, *91*, 5977–5983.

44. Lever, A.P.B. *Inorganic Electronic Spectroscopy*, 2nd ed.; Elsevier Science: New York, NY, USA, 1984.
45. John, R.P.; Sreekanth, A.; Rajakannan, V.; Ajith, T.A.; Kurup, M.R.P. New copper(II) complexes of 2-hydroxyacetophenone N(4)-substituted thiosemicarbazones and polypyridyl co-ligands: Structural, electrochemical and antimicrobial studies. *Polyhedron* **2004**, *23*, 2549–2559.
46. Wilkinson, G.; Gillard, D.R.; McCleverty, A.J. *Comprehensive Coordination Chemistry*; Pergamon Press: New York, NY, USA, 1987; pp. 3–5.
47. Carlin, R.L. *Transition Metal Chemistry*, 2nd ed.; Marcel Decker: New York, NY, USA, 1965.
48. Zanello, P.; Tamburini, S.; Vigato, P.A.; Mazzocchin, G.A. Syntheses, structure, and electrochemical characterization of homo- and heterodinuclear copper complexes with compartmental ligands. *Coord. Chem. Rev.* **1987**, *77*, 165–273.
49. Guerriero, P.; Tamburini, S.; Vigato, P.A. From mononuclear to polynuclear macrocyclic or macroacyclic complexes. *Coord. Chem. Rev.* **1995**, *139*, 17–243.
50. Yu, J.W.; Tao, R.J.; Zhou, X.Y.; Jui, D.M.; Liao, D. Syntheses and magnetic properties of heterobinuclear complexes with N,N'-bis(3-carboxylsalicylidene)trimethylenediamine. *Polyhedron* **1994**, *13*, 951–955.
51. Lam, F.; Wang, R.J.; Mak, T.C.W.; Chan, K.S. Synthesis of novel dinickel(II) and nickel(II)-copper(II) bimetallic complexes derived from an acyclic dinucleating Schiff base-pyridine ligand. *J. Chem. Soc. Chem. Commun.* **1994**, *21*, 2439–2440.
52. Benzekri, A.; Dubourdeaux, P.; Latour, J.M.; Rey, P.; Laugier, J. Binuclear copper(II) complexes of a new sulphur-containing binucleating ligand: Structural and physicochemical properties. *J. Chem. Soc. Dalton Trans.* **1991**, *12*, 3359–3365.
53. Kettle, S.F.A. *Physical Inorganic Chemistry Approach*; Oxford University Press: Oxford, UK, 1998.
54. Anderson, P.W. Antiferromagnetism. Theory of Superexchange Interaction. *Phys. Rev.* **1950**, *79*, 350–352.
55. Hathaway, B.J.; Billing, D.E. The electronic properties and stereochemistry of mononuclear complexes of the copper(II) ion. *Coord. Chem. Rev.* **1970**, *5*, 143–207.
56. Bew, M.J.; Hathaway, B.J.; Faraday, R.R. Electronic properties and stereochemistry of the copper(II) ion. Part VII. Mono(diethylenetriamine)copper(II) complexes. *J. Chem. Soc. Dalton Trans.* **1972**, *12*, 1229–1237.
57. Siegel, I.; Jones, E.P. Electronic bonding of Cu^{2+} in amorphous and crystalline TeO_2 : EPR and optical spectra. *J. Chem. Phys.* **1972**, *57*, 2364–2371.
58. Maki, A.H.; McGarvey, B.R. Electron spin resonance in transition metal chelates. I. Copper (II) bis-acetylacetonate. *J. Chem. Phys.* **1958**, *29*, 31.
59. Kivelson, D.; Neiman, R. ESR studies on the bonding in copper complexes. *J. Chem. Phys.* **1961**, *35*, 149–155.
60. Hathaway, B.J. *Structure and Bonding*; Springer Verlag: Heidelberg, Germany, 1973; p. 60.
61. Hathaway, B.J. *Comprehensive Coordination Chemistry*; Wilkinson, G., Gillard, D.R., McCleverty, A.J., Eds.; Pergamon Press: New York, NY, USA, 1987.

62. Barry, A. Procedures and theoretical considerations for testing antimicrobial agents in agar media. In *Antibiotics in Laboratory Medicine*, 5th ed.; Lorian, A., Ed.; Williams and Wilkins: Baltimore, MD, USA, 1991.
63. National Committee for Clinical Laboratory Standard. *NCCLS: Methods for Antimicrobial Dilution and Disk Susceptibility Testing of Infrequently Isolated or Fastidious Bacteria, Approved Guideline*; Document M45-A, 26(19); NCCLS: Willanova, PA, USA, 1999.
64. *CrysAlis RED*, Version 1.171.36.32; Oxford Diffraction Ltd.: Abingdon, UK, 2003.
65. Dolomanov, O.V.; Bourhis, L.J.; Gildea, R.J.; Howard, J.A.K.; Puschmann, H. Olex2: A complete structure solution, refinement and analysis program. *J. Appl. Crystallogr.* **2009**, *42*, 339–341.
66. Sheldrick, G.M. A short history of SHELXS. *Acta Crystallogr. A* **2008**, *64*, 112–122.
67. Samusi, N.; Prisacari, V.; Tapcov, V.; Buraciov S. Di(μ -O)di[N-(2-oxo-1-naftali)-N1- α -oxobenzalhidrazincopper] Dihidrate, Which Have Selective Antibacterien Activity. Patent of Invention MD 678 BOPI, 1997.
68. Samusi, N.M.; Prisacari, V.I.; Tapcov, V.I.; Buraciov, S.A.; Gulea, A.P. Synthesis and antimicrobial activity of the complexes of 3d-metals with substituted salicylaldehyde benzoylhydrazones. *Pharm. Chem. J.* **2004**, *38*, 373–377.
69. Gulea, A.P.; Samusi, N.M.; Prisacari, V.I.; Tapcov, V.; Buraciov, S.A.; Spinu, S.N.; Begenari, N.P.; Poirier, D.; Roy, J. Synthesis and antimicrobial activity of sulfanylamide-containing copper(II) and nickel(II) salicylidene thiosemicarbazidates. *Pharm. Chem.* **2007**, *41*, 596–599.

Sample Availability: Not available.

© 2015 by the authors; licensee MDPI, Basel, Switzerland. This article is an open access article distributed under the terms and conditions of the Creative Commons Attribution license (<http://creativecommons.org/licenses/by/4.0/>).